

See discussions, stats, and author profiles for this publication at: <https://www.researchgate.net/publication/263958219>

# Combustion Behavior of Algal Biomass: Carbon Release, Nitrogen Release, and Char Reactivity

ARTICLE *in* ENERGY & FUELS · NOVEMBER 2013

Impact Factor: 2.79 · DOI: 10.1021/ef4014983

CITATIONS

13

READS

62

8 AUTHORS, INCLUDING:



[Peter J. Ashman](#)

University of Adelaide

81 PUBLICATIONS 690 CITATIONS

[SEE PROFILE](#)



[Mikko Markus Hupa](#)

Åbo Akademi University

426 PUBLICATIONS 5,476 CITATIONS

[SEE PROFILE](#)



[Oskar Karlström](#)

Åbo Akademi University

15 PUBLICATIONS 70 CITATIONS

[SEE PROFILE](#)



[David M Lewis](#)

University of Adelaide

68 PUBLICATIONS 748 CITATIONS

[SEE PROFILE](#)

# Combustion Behavior of Algal Biomass: Carbon Release, Nitrogen Release, and Char Reactivity

Daniel J. Lane,<sup>†</sup> Peter J. Ashman,<sup>\*,†</sup> Maria Zevenhoven,<sup>‡</sup> Mikko Hupa,<sup>‡</sup> Philip J. van Eyk,<sup>†</sup> Rocky de Nys,<sup>§</sup> Oskar Karlström,<sup>‡</sup> and David M. Lewis<sup>†</sup>

<sup>†</sup>School of Chemical Engineering, University of Adelaide, Adelaide, South Australia 5005, Australia

<sup>‡</sup>Process Chemistry Centre, Åbo Akademi University, Piispankatu 8, 20500 Turku, Finland

<sup>§</sup>School of Marine and Tropical Biology, James Cook University, Townsville, Queensland 4811, Australia

**ABSTRACT:** Recent focus on algae biomass as an alternative energy source can be attributed to building pressure for conservation of dwindling fossil fuels and reduced greenhouse gas emissions. Both micro- and macroalgae have many advantages over terrestrial plants, including typically faster growth rates and, therefore, higher rates of carbon fixation. This paper reports the combustion characteristics of a species of microalgae and two species of macroalgae under conditions that are relevant for the large-scale use of biomass for heat and other products. The tested species were *Tetraselmis* sp. (marine microalgae), *Derbersia tenuissima* (marine macroalgae), and *Oedogonium* sp. (freshwater macroalgae). Two variants of *Oedogonium* were tested. One variant was cultivated using standard nutrient additions, and the other variant was starved of essential nutrients. Carbon conversion to CO and CO<sub>2</sub> and the release of N as NO were determined for the algae by oxidizing fixed-bed samples of each alga in air at 800 and 1000 °C. The gasification reactivity of the chars was also characterized by gasifying samples of each alga in a thermobalance in pure CO<sub>2</sub> (1 atm) at 800 °C, following *in situ* devolatilization of the algal samples. Carbon conversion to CO and CO<sub>2</sub> exceeded 84% for all of the tested algae. Most of the fuel C was released during fuel devolatilization, consistent with the proximate analysis for these fuels. Nitrogen conversions to NO ranged between 6 and 12 g of N/100 g of fuel N for *Tetraselmis*, 6–9 g of N/100 g of fuel N for *Derbersia*, and 11–21 g of N/100 g of fuel N for the two *Oedogonium* variants, with NO emissions occurring mainly during devolatilization, in most cases. Chars produced from samples of macroalgae were much more reactive than the chars from the microalgae, most likely because of the inhibitory effects on mass transfer caused by the very high ash content of the sample used in the present study. The reactivities of all chars increased at high char conversions.

## 1. INTRODUCTION

Declining fossil fuel reserves and concerns regarding both future fuel security and the environmental impacts associated with greenhouse gas emissions provide strong motivation to develop alternative fuel technologies based on the sustainable use of plant biomass.<sup>1</sup> Combustion is one possible conversion pathway to energy that is already widely used for terrestrial biomass, and this process is well-understood for many common fuels. There have been numerous investigations of the combustion behavior of terrestrial feedstocks, ranging from woody biomass<sup>2–5</sup> to various sources of waste-derived fuels.<sup>6–10</sup>

Algae have received much attention recently because these plants are promising sources of biomass, which have several advantages over terrestrial plants. Algae have excellent potential for high energy yields per unit of land area. Productivities as high as 50 g m<sup>-2</sup> day<sup>-1</sup> are commonly reported in the literature.<sup>11,12</sup> Algae can be cultivated in fresh<sup>13</sup> to hypersaline water,<sup>14</sup> and unlike other plants, its production does not require arable land.<sup>15</sup> Expensive nutrient inputs can also be avoided by growing algae in agricultural,<sup>16</sup> municipal,<sup>17</sup> and industrial wastewater,<sup>18</sup> thus avoiding direct competition for nutrients with food crops.

Any new feedstock must be adequately characterized to identify the main challenges and benefits associated with its use as a fuel, and limited work has been performed previously to characterize the combustion behavior of algae. The literature

focuses mainly on a limited range of more conventional fuel analyses<sup>13,19–27</sup> for a small range of algae species grown under a limited range of conditions. Proximate, ultimate, ash elemental, and heating value analyses are usually performed as a first step when characterizing new fuels. The results of these fuel analyses will vary quite widely for algae from species to species and likely depend upon a range of growing conditions, including the availability of nutrients. Often the minimization of nutrient addition is a key objective in the production of algae, and this is expected to influence the fuel properties of the resultant biomass. It is an aim of this work to investigate the extent to which different levels of nutrient addition affect the combustion behavior of algae.

Algae are typically high in elemental nitrogen, with nitrogen contents usually reported between 0.8 and 4.5 wt %<sup>20,23,27</sup> for macroalgae and between 6.7 and 10.3 wt %<sup>21,22,25,26</sup> for microalgae, on a dry and ash-free (daf) basis. Nitric oxide (NO), which may be formed from fuel N, is a harmful pollutant<sup>28</sup> that is a precursor to photochemical smog.<sup>29</sup> Emissions of nitrogen oxides (NO<sub>x</sub>) are typically highly

**Special Issue:** 4th (2013) Sino-Australian Symposium on Advanced Coal and Biomass Utilisation Technologies

**Received:** July 31, 2013

**Revised:** October 21, 2013

**Published:** October 23, 2013



regulated<sup>28</sup> and have motivated<sup>28</sup> a vast amount of research aimed at understanding the conversion of fuel-bound N, which at low temperatures is generally the dominant contributor to NO<sub>x</sub> emissions.<sup>28</sup> There have been numerous investigations into the release of fuel N from coal<sup>30,31</sup> and from terrestrial biomass,<sup>32–35</sup> and these show that mechanisms of NO<sub>x</sub> formation differ depending upon whether fuel N is released during devolatilization or during char oxidation; thus, in practical systems, effective control measures to reduce NO<sub>x</sub> emissions will depend upon the degree of partitioning between volatile N and char N. Ross et al.<sup>20</sup> compared the decomposition of six macroalgae to three different types of terrestrially sourced biomass during flash pyrolysis using thermogravimetric analysis (TGA), differential thermal analysis (DTA), and pyrolysis–gas chromatography–mass spectrometry (Py–GC–MS). They reported a greater release of nitrogenous compounds from the macroalgae and suggested that the fate of these compounds could be problematic in combustion systems. Limited work has been performed to understand the release of nitrogen during the combustion of algae.

Fuel reactivity affects the extent of fuel conversion in industrial combustion and gasification reactors and, therefore, is an important element of fuel characterization. When a solid fuel particle is fed to an industrial reactor, volatile components in the organic matter are released during pyrolysis, while the residual char is converted via much slower heterogeneous reactions with gas-phase reactants. The reactivity of the residual char depends upon not only the devolatilization conditions but also the intrinsic nature of the fuel. Furthermore, the performance of the combustion process will be strongly influenced by the relative amounts of volatiles and char. Terrestrial biomass is typically high in volatile matter,<sup>36</sup> and therefore, most of the carbon in the fuel is released during devolatilization. A similar behavior could be expected from algae given the high volatile matter contents reported in the literature for these fuels (58–84 wt %, daf).<sup>20,23,24</sup> A few experimental studies<sup>20,37</sup> have investigated the decomposition of algae during combustion; however, they all used slow heating rates, which poorly resemble conditions inside industrial reactors where heating of the fuel particles is rapid. No studies have been performed to track the conversion of carbon during algae combustion.

The reactivity of the residual char is especially important in determining the total conversion of carbon. There have been numerous studies focusing on the reactivity of terrestrial biomass chars and the factors that contribute to their reactivity. It is well-known from experience gasifying chars from coal<sup>38,39</sup> and terrestrial biomass<sup>40,41</sup> that the ash plays a key role in determining the reactivity of the char as well as influencing other operational factors, such as fouling,<sup>42</sup> during combustion and gasification. Ash interactions with the surrounding gaseous environment and with the char can act to catalyze or suppress char reactivity.<sup>40</sup> Algae typically contain large amounts of ash<sup>19–21,23,24</sup> and usually contain significant levels of Na, K, Ca, Mg, and Si,<sup>20,23</sup> and the alkali metals, in particular, are known to catalyze char gasification.<sup>38,40,41</sup> The alkaline earth metals have also been reported<sup>38,39</sup> to play a catalytic role but to a lesser extent than the alkali metals.<sup>39</sup> Silicon, on the other hand, has been reported to inhibit char gasification through the formation of inactive alkali silicates.<sup>40</sup> The overall catalytic influence of the ashes is likely to depend upon the balance of the main ash-forming elements in algae. Kirtania et al.<sup>43</sup> compared the

gasification reactivity of *Chlorella* sp., a species of microalgae, to that of a commercial wood mix by monitoring weight loss during the gasification of two chars prepared from these two fuels. The chars were prepared in both an entrained flow reactor and a thermogravimetric analyser with two different gasifying agents and at two different temperatures. They found<sup>43</sup> chars prepared from the wood mix to be more reactive than the microalgae chars under most conditions. No other studies have been performed to characterize the reactivity of algal chars or understand how reactivity varies between species and with different growth conditions.

Therefore, the aim of this study was to characterize the combustion behavior of algal biomass. The specific objectives were to characterize the release of fuel N, the conversion of carbon, and the gasification reactivity of the chars for a range of algae species and different nutrient addition strategies.

## 2. EXPERIMENTAL SECTION

**2.1. Algae Species.** A diverse range of algae types were selected for this work to partly assess the variability in the combustion behavior of algal biomass for different types of species with different growing conditions. The experimental framework included micro- and macroalga species, freshwater and marine species, and two variants of the same species grown under different nutrient addition regimes. One species of microalgae (*Tetraselmis* sp.) and two species of macroalgae (*Derbesia tenuissima* and *Oedogonium* sp.) were studied in this work. In addition, two variants of *Oedogonium* were studied. One variant was cultivated using standard nutrient additions, and the other variant was starved of essential nutrients.

The *Tetraselmis* biomass (hereafter referred to as “Tet”) used in this work was grown in an outdoor 20 m<sup>2</sup> raceway pond. The culture was grown in seawater and harvested every second day by electro-flocculation followed by centrifugation. The electroflocculation process involves the application of an electric current to sacrificial aluminum electrodes, which supply ions required for flocculation. The flocs, which are bubbled to the surface of the water column by gas bubbles formed at the electrodes, are then collected by skimming. The product biomass from each harvest was frozen prior to storage. Before use, samples were thawed and then oven-dried (45 °C) to a moisture content of less than 10 wt %. While individual *Tetraselmis* cells are of the order of 10 μm in size,<sup>44</sup> during drying, the cells aggregate to form brittle clusters up to 20 mm in size.

The *Derbesia* biomass, *D. tenuissima* (Chlorophyta, Bryopsidales) (hereafter referred to as “Deb”), was cultured in 2500 L tanks at James Cook University (JCU), Townsville, Queensland, Australia. The tanks were stocked at 1 g L<sup>-1</sup> in filtered seawater (3.5 wt %) with f/2 media and harvested every 7 days by filtration through mesh bags (0.1 mm), which were subsequently spun dry (Fisher and Paykell). Harvested biomass was combined and washed in freshwater prior to being spun dry and then dried in a solar kiln (60 °C) to a moisture content of less than 10 wt %. The dried biomass consisted of tufts of intertwined filaments. The mean length and width of the dried filaments (±1 standard deviation) were measured using an optical microscope as 7.6 ± 2.9 and 0.026 ± 0.004 mm, respectively.

The *Oedogonium* biomass (*Oedogonium* from the *Crispum* group<sup>13</sup>) was cultured in 15 000 L rectangular tanks at JCU, Townsville, Queensland, Australia. The tanks were stocked at 0.5 g L<sup>-1</sup> in dechlorinated water with microalgae food (MAF) culture media (0.1 g L<sup>-1</sup>) and harvested after 7 days by filtration through mesh bags (0.1 mm), which were subsequently spun dry (Fisher and Paykell). This high nitrogen biomass (hereafter referred to as “OD + N”) was divided, and a proportion was retained and air-dried until the moisture content was less than 10 wt %. The remaining *Oedogonium* biomass was stocked at an initial density of 0.5 g L<sup>-1</sup> into 2500 L tanks with bore water without the addition of nutrients. This low nitrogen biomass (hereafter referred to as “OD – N”) was harvested after 7 days as above and air-dried until the moisture content was less than 10 wt %. The dried *Oedogonium* biomass consisted of tufts of intertwined

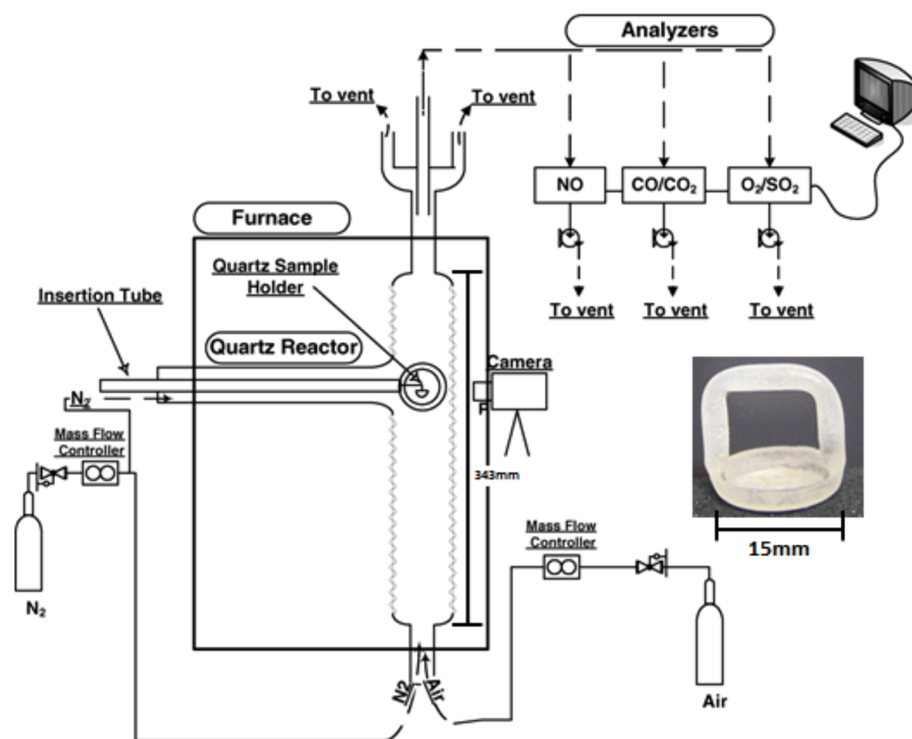


**Figure 1.** Quartz furnace setup at Åbo Akademi University (taken from Giuntoli et al.<sup>33</sup>) and (inset) photograph of one of the quartz sample holders.

filaments, similar in appearance to Deb. The mean length and width of the dried filaments ( $\pm 1$  standard deviation) were measured using an optical microscope as  $4.6 \pm 0.9$  and  $0.03 \pm 0.002$  mm, respectively.

Representative samples of each species of macroalgae were milled using a centrifugal knife mill and then sieved to pass through a 1 mm screen to obtain particles that were approximately similar in size to the microalgae particles. The dried microalgae was also sieved through a 1 mm screen to remove coarse particles. The action of sieving alone was sufficient to break most of the coarse microalgae clusters. The resultant biomass was split by cone and quartering to obtain smaller sample sizes for each analysis.

**2.2. Experiments.** Conventional fuel analyses were performed on each alga sample. Ultimate, proximate, ash elemental, and heating value analyses were performed externally by Belab AB and ALS Scandinavia (accredited laboratories in Sweden) according to Swedish standards. Elemental C, H, and N were determined according to SS-EN 15104:2011/15407:2011. Elemental O was calculated by difference. Elemental S and the ash analyses were determined using modified United States Environmental Protection Agency (U.S. EPA) methods 200.7 [inductively coupled plasma–atomic emission spectrometry (ICP–AES)], 200.8 [inductively coupled plasma–mass spectrometry (ICP–MS)], and 200.8 [inductively coupled plasma–sector field mass spectrometry (ICP–SFMS)]. Moisture and volatile matter contents were determined according to SS028113-1 and SS-EN 15148:2009/15402:2011, respectively. Fixed carbon was calculated by difference. Heating values were determined according to 14918:2010/15400:2011.

**2.2.1. Carbon and Nitrogen Release Experiments.** The carbon release as CO and CO<sub>2</sub> and N release as NO were characterized by oxidizing samples of the algae in a lab-scale quartz furnace at Åbo Akademi University.

**2.2.1.1. Apparatus Setup.** A schematic of the quartz furnace setup is shown in Figure 1. The setup consisted of an insulated quartz tube reactor (inner diameter of 44 mm) connected to a series of commercial gas analysers. A chemiluminescence analyzer was used for NO measurement and a non-dispersive infrared analyzer for simultaneous CO and CO<sub>2</sub> measurements. The setup did not allow for the measurement of light hydrocarbons (e.g., CH<sub>4</sub>) or for the measurement of nitrogenous species other than NO. A view port at

the front of the reactor, designed for video recording, allowed for visual observation. Samples were fed into the reactor using a quartz sample holder suspended from the end of a quartz insertion probe. The feeding system was designed such that the sample could be preserved in N<sub>2</sub> and maintained at close to ambient temperature while conditions inside the furnace stabilized. Once the conditions inside the furnace had stabilized, the sample was inserted into the reactor within a fraction of a second. Dry air and N<sub>2</sub> were fed into the front, bottom, and side of the reactor to create the desired gas atmosphere. Mixing of the gases occurred inside the reactor. Mass flow controllers were used to control the flows of each gas to the different locations. The total gas flow into the reactor was kept constant at 220 L h<sup>-1</sup> [standard temperature and pressure (STP)]. This flow rate allowed for sufficient time for the incoming gases to be heated to the reactor temperature. It also resulted in a relatively short transfer time of the product gases between the reactor and the gas analysers, which was estimated to be around 4 s. Four externally controlled electric heating elements were used to heat the furnace. The heating elements were distributed evenly around the outside of the quartz tube to provide uniform heating. A K-type thermocouple, located just beneath the base of the quartz tube, was used for temperature measurement inside the reactor.

**2.2.1.2. Procedure.** Samples of milled alga (10–15 mg) were loaded onto the quartz sample holder to create a thin layer of particles with a depth no greater than 2 mm. The samples were oxidized at the following three sets of conditions: 3% O<sub>2</sub> and 800 °C, 10% O<sub>2</sub> and 800 °C, and 10% O<sub>2</sub> and 1000 °C. The concentrations of NO, CO, CO<sub>2</sub>, and O<sub>2</sub> in the product gases from the furnace were measured during each test. Tests were repeated at least 4 times at each condition to assess the reproducibility of the measurements. The tests showed reasonable reproducibility: the relative standard deviations of the integrals of the CO + CO<sub>2</sub>, NO, and O<sub>2</sub> curves were usually within 6, 11, and 5%, respectively. The average integral of the measured signals was calculated to determine the conversion of fuel C to CO and CO<sub>2</sub> and the total release of fuel N as NO. A representative signal from each test was selected to partition the total release of carbon and fuel N as NO between fuel devolatilization and oxidation of the residual char. The representative signal was deconvolved using a standard Matlab routine, which used the residence time distributions (RTDs) of the



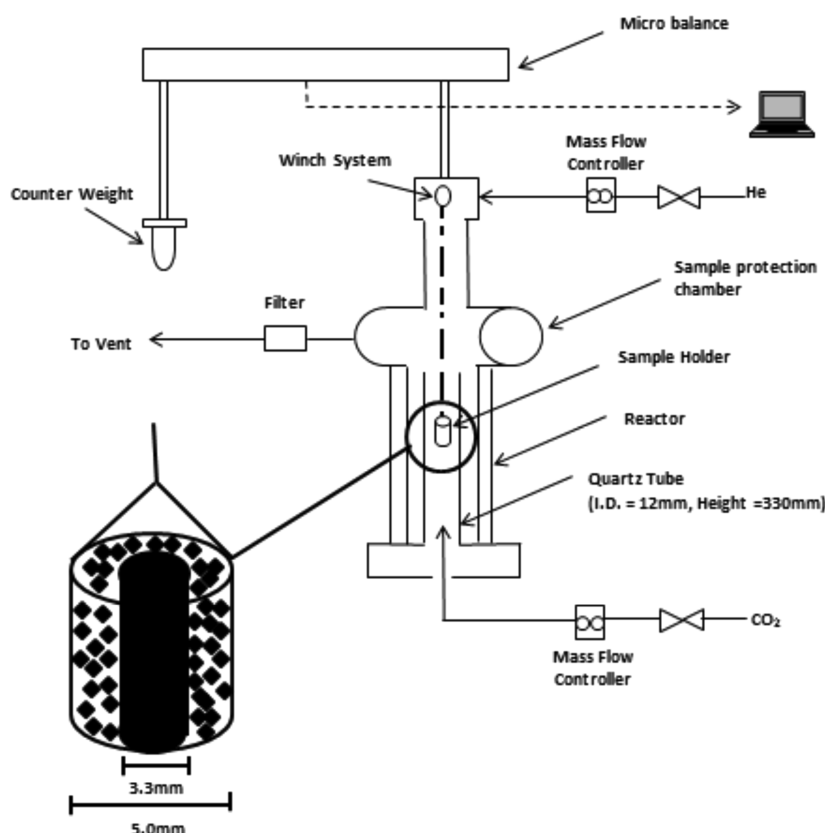


Figure 2. Simplified schematic of the experimental setup used in the char reactivity experiment.

Table 1. Proximate, Ultimate, and Heating Value Analyses of the Tested Algae<sup>a</sup>

	Tet	Deb	OD + N	OD - N	spruce wood <sup>36,45</sup>	switchgrass <sup>36,46</sup>	chicken manure <sup>47</sup>	sewage sludge <sup>36,48</sup>
Proximate (wt %)								
moisture <sup>b</sup>	7.9	6.6	6.2	8.2				
VM <sup>c,d</sup>	41.9	74.8	77.3	77.2	81.1	80.4	67.9	48.1
FC <sup>e,d</sup>	<1.0	15.1	14.7	6.1	18.3	14.5	5.5	5.7
ash	64.4	10.1	8.0	16.7	0.5	5.1	26.6	46.2
Ultimate (wt %) <sup>f</sup>								
C	42.1	52.6	49.1	47.4	52.3	49.7	54	50.9
H	8.7	7.2	6.8	6.8	6.1	6.1	5.6	7.3
N	6.7	7.6	4.5	1.5	0.3	0.7	8	6.1
O	35.4	30.9	39.2	44.1	41.2	43.4	30.9	33.4
S	6.9	1.3	0.12	0.20	0.1	0.11	1	2.33
higher heating value (MJ/kg) <sup>f</sup>	15.5	21.7	19.36	17.39	20.1	18.6	18.1	20.8

<sup>a</sup>The analyses are compared to the analyses of terrestrial biomass reported in the literature. <sup>b</sup>After drying. <sup>c</sup>Volatile matter. <sup>d</sup>Dry basis. <sup>e</sup>Fixed carbon. <sup>f</sup>Dry and ash-free basis.

measured gas species as an input. Step tests were performed with CO, CO<sub>2</sub>, and NO to determine RTDs.

**2.2.2. Char Reactivity Experiment.** The gasification reactivities of the algal chars were characterized by gasifying samples of each alga in a pure CO<sub>2</sub> environment (1 atm) at 800 °C in a thermogravimetric analyser at Åbo Akademi University. A simplified schematic of the TGA setup is shown in Figure 2. The method used was adapted from a method developed by Moilanen<sup>40</sup> to characterize the reactivity of terrestrial biomass chars. The method involves *in situ* drying and devolatilization of the fuel sample, simulating conditions in an industrial reactor. Samples of each alga (35–182 mg) were packed into an inconel sample holder, which was then held above a quartz tube furnace in an inert water-cooled gas chamber, while the furnace was heated to 800 °C. The sample holder consisted of a solid cylinder surrounded by porous wire mesh. The sample was packed into the annular region between the wire mesh and the cylinder. The sample

layer was sufficiently thin (<1.7 mm) to promote good contact with the gasifying agent. Once the furnace temperature reached 800 °C, the sample was lowered into the furnace using an electrically operated winch. A total of 27 s was required to lower the sample into the furnace and for the balance to stabilize. The sample weight was recorded from 27 s up until steady-state weight was obtained with a sampling interval of 0.5 s. A K-type thermocouple located just beneath the sample holder was used to monitor the furnace temperature. Helium was fed at a rate of 2.2 L min<sup>-1</sup> to the inert chamber and preheated CO<sub>2</sub> at a rate of 2.0 L min<sup>-1</sup> to the bottom of the furnace. Gas flows were controlled using mass flow controllers.

The obtained weight loss curves were used to calculate the rate profiles for char gasification. The rate profiles show the instantaneous reaction rate as a function of char conversion. In this work, the instantaneous rate was defined as the rate of mass change of the char divided by the mass of residual ash-free char and char conversion was

defined as the reacted part of the ash-free char. The instantaneous rate,  $r''$  ( $\text{min}^{-1}$ ), was calculated according to eq 1, and char conversion,  $X$  (%), was calculated according to eq 2

$$r'' = \frac{-(m_i - m_{i-1})}{(t_i - t_{i-1})(m_i - m_F)} \quad (1)$$

$$X = 1 - \frac{m_i - m_F}{m_0 - m_F} \quad (2)$$

where  $m_i$  is the sample mass at time  $t_i$ ,  $m_{i-1}$  is the sample mass at time  $t_{i-1}$ ,  $m_F$  is the minimum sample mass, and  $m_0$  is the initial mass of char, which was approximated by the sample mass at the time corresponding to a sudden reduction in the slope of the weight loss curve. This point is assumed to correspond to the end of fuel devolatilization and the onset of char gasification.

### 3. RESULTS AND DISCUSSION

The results from the proximate, ultimate, and heating value analyses are presented in Table 1, and the results from the ash elemental analyses are presented in Table 2. Data for four

**Table 2. Ash Elemental Analyses for the Tested Algae**

	mg/kg of dry biomass			
	Tet	Deb	OD + N	OD - N
Na	110000	14300	2280	2890
K	8090	9250	14900	21800
Ca	19400	2600	2680	22700
Mg	19500	5850	2920	10100
Si	5910	3470	10400	12600
P	1930	4530	6840	2130
Al	65100	113	710	793
Fe	996	833	2280	627
Ti	81.4	12.6	28.4	29.6
Mn	43.1	38	279	216
Cl	182000	19800	2380	7930

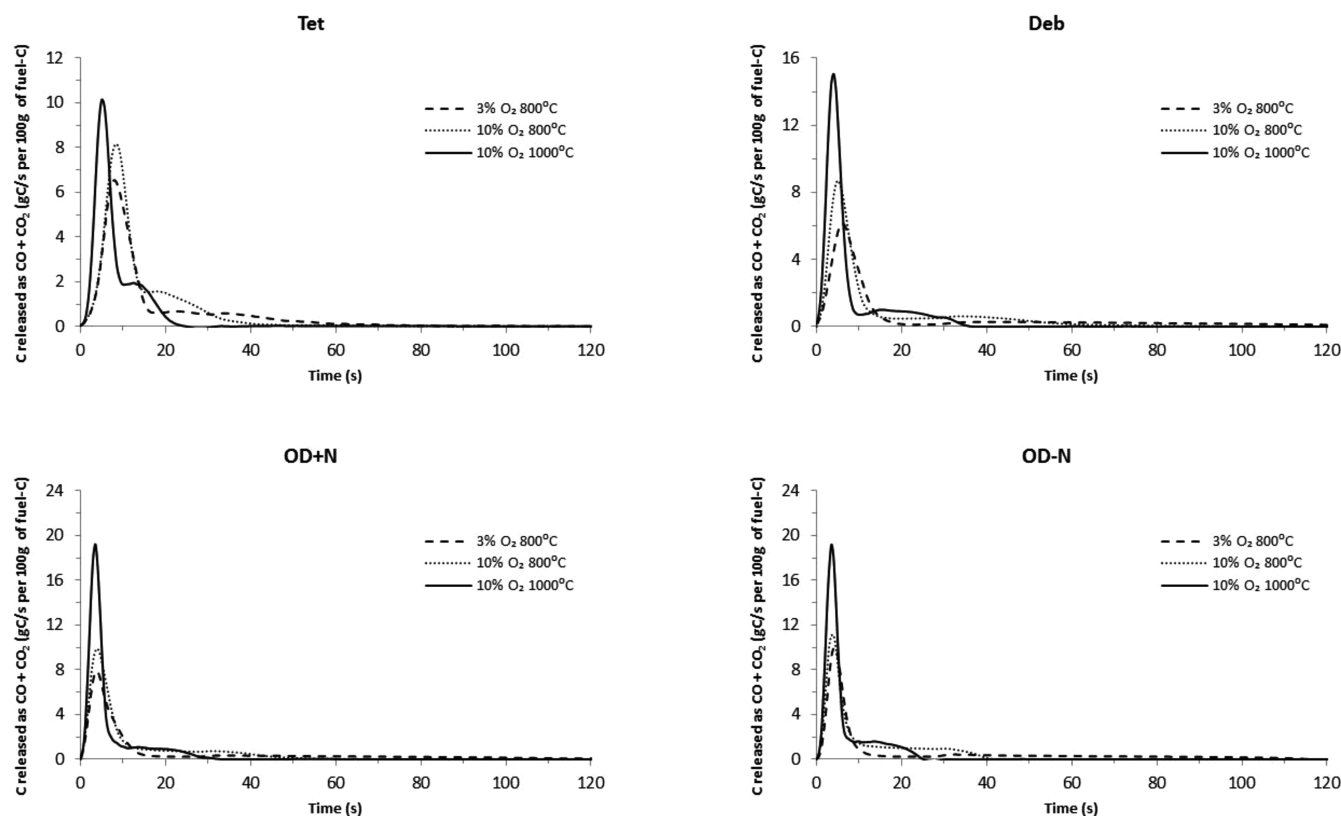
terrestrial biomass fuels, viz., spruce wood,<sup>36,45</sup> switchgrass,<sup>36,46</sup> chicken manure,<sup>47</sup> and sewage sludge,<sup>36,48</sup> have also been included in Table 1 for comparison. The *Derbersia* biomass (Deb) and the high-nitrogen *Oedogonium* biomass (OD + N) have the highest fixed carbon (FC) of the tested algae on a daf basis with 16.8 and 16.0 wt %, respectively. The ratio of volatile matter (VM) to FC in Deb and OD + N are approximately 5 and are typical of that reported for grasses.<sup>36,46</sup> The low-nitrogen *Oedogonium* biomass (OD - N) contained similar proportions of FC and VM to chicken manure and approximately half as much FC as OD + N on a daf basis. The lack of essential nutrients available to OD - N during its growth has likely caused changes to the biochemical structure of the plant material, which has resulted in a greater proportion of the organic matter being released as VM during devolatilization. The *Tetraselmis* biomass (Tet) was reported to contain less than 3 wt % FC (daf) based on the standard analytical method used for this analysis. This value is very low and is much lower than what is reported for terrestrial plants in a recent overview<sup>36</sup> of the chemical composition of over 80 types of biomass. Furthermore, our own determination of the FC content using a thermogravimetric analyser, albeit under different conditions to the standard method, showed the FC content of the Tet sample to be approximately 9 wt %, which is also supported by observations from our own combustion experiments. It is possible that the discrepancy between the two analyses is due to some organic material remaining unconverted

in the standard method. The Tet sample has a very high ash content (64.4 wt %), and it is possible that mass transfer resistance caused by the formation of a substantial ash layer in the Tet sample prevents the complete conversion of the Tet sample. Nevertheless, the FC content of Tet is clearly lower than that measured for other algae and can be attributed to the structural simplicity of microalgae.

The ash contents of the tested algae were in the range of 8.0–64.4 wt % on a dry basis (db) and varied substantially between species. Differences in the growth and harvesting processes used to produce the different types of algae biomass are expected to account for much of this variation. Tet had the highest ash content (64.4 wt %) followed by OD - N (16.7 wt %), Deb (10.1 wt %), and then OD + N (8.0 wt %). The difference in the ash contents of OD + N and OD - N is attributable to the final culture of OD - N occurring in bore water, which was high in carbonates, resulting in internal accumulation of salts and, therefore, ash. The composition of ashes from both the marine algae, Tet and Deb, are dominated by NaCl originating from the seawater in which they were cultured. The lower ash content of Deb compared to Tet is due to Deb being washed with freshwater prior to drying. The extremely high ash content of the Tet sample is attributed to the hypersaline growth conditions but also the harvesting and drying processes employed. The electroflocculation harvesting process, which causes flocculation and flotation of microalgae, may also recover other fine materials present in the pond. While this biomass sample was partially dewatered using centrifugation, the Tet samples were finally dried by evaporation, resulting in a concentration of soluble inorganic matter associated with the water phase of the wet biomass.

The elemental composition of OD + N and OD - N (Table 1) was similar and also similar to that of switchgrass<sup>36</sup> on a daf basis, except that OD + N contained higher levels of N. Deb had a higher C content and significantly lower O content (8–13%) than the two variants of *Oedogonium*. Thus, Deb had the highest calorific value, despite it containing more ash than OD + N. The elemental composition of Deb was similar to that of chicken manure<sup>47</sup> on a daf basis. Tet contained high levels of both N and S and contained the least C of the algae tested. The S levels in Tet are 4–13 times higher than those reported in the literature<sup>21,22,25,26</sup> for microalgae laboratory cultures. It is suspected but not confirmed that extraneous sulfate ions were incorporated within the biomass during the electroflocculation harvesting process. Deb also had a higher S content (1.3 wt %) than the two *Oedogonium* variants (0.1–0.2 wt %).

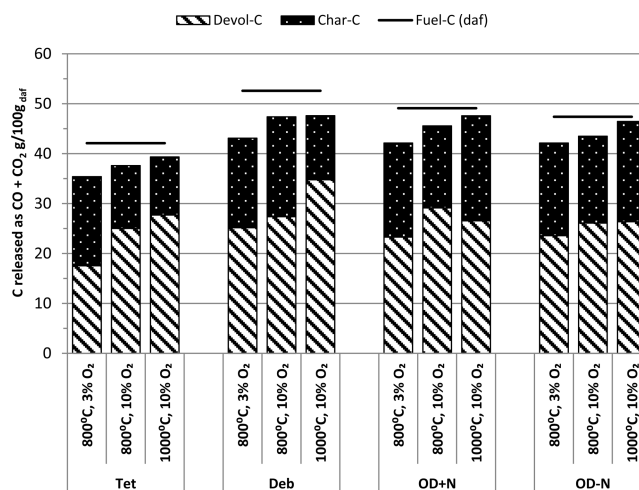
Nitrogen levels in the tested algae ranged between 1.5 and 7.6 wt % (daf). The N content of Tet was 6.7 wt %, which is at the lower limit of that reported in the literature<sup>21,22,25,26</sup> for microalgae. The high levels of N in microalgae are attributed to the ability of microalgae to store excess N as nitrate in their vacuoles.<sup>49</sup> OD - N contained 1.5 wt % N, the lowest of all of the algae tested here, and this value is typical of grasses<sup>36</sup> and herbaceous crops.<sup>36</sup> OD + N contained 4.5 wt % N, which is 3 times more than that in OD - N. This was expected given that OD - N was starved of N during cultivation. The highest N content was measured for Deb (7.6 wt %, daf). Given the high levels of N in Deb and OD + N, it is likely that these two macroalgae stored excess N to what is needed for essential biological functioning (luxury uptake). In contrast, it is expected that a large part of the N in OD - N was incorporated into essential organic molecules, such as proteins.



**Figure 3.** Carbon released as CO and CO<sub>2</sub> from the tested algae in a quartz tube furnace. Release profiles obtained at 10 vol % O<sub>2</sub> and 800 °C are compared to release profiles obtained at 3 vol % O<sub>2</sub> and 800 °C and at 10 vol % O<sub>2</sub> and 1000 °C.

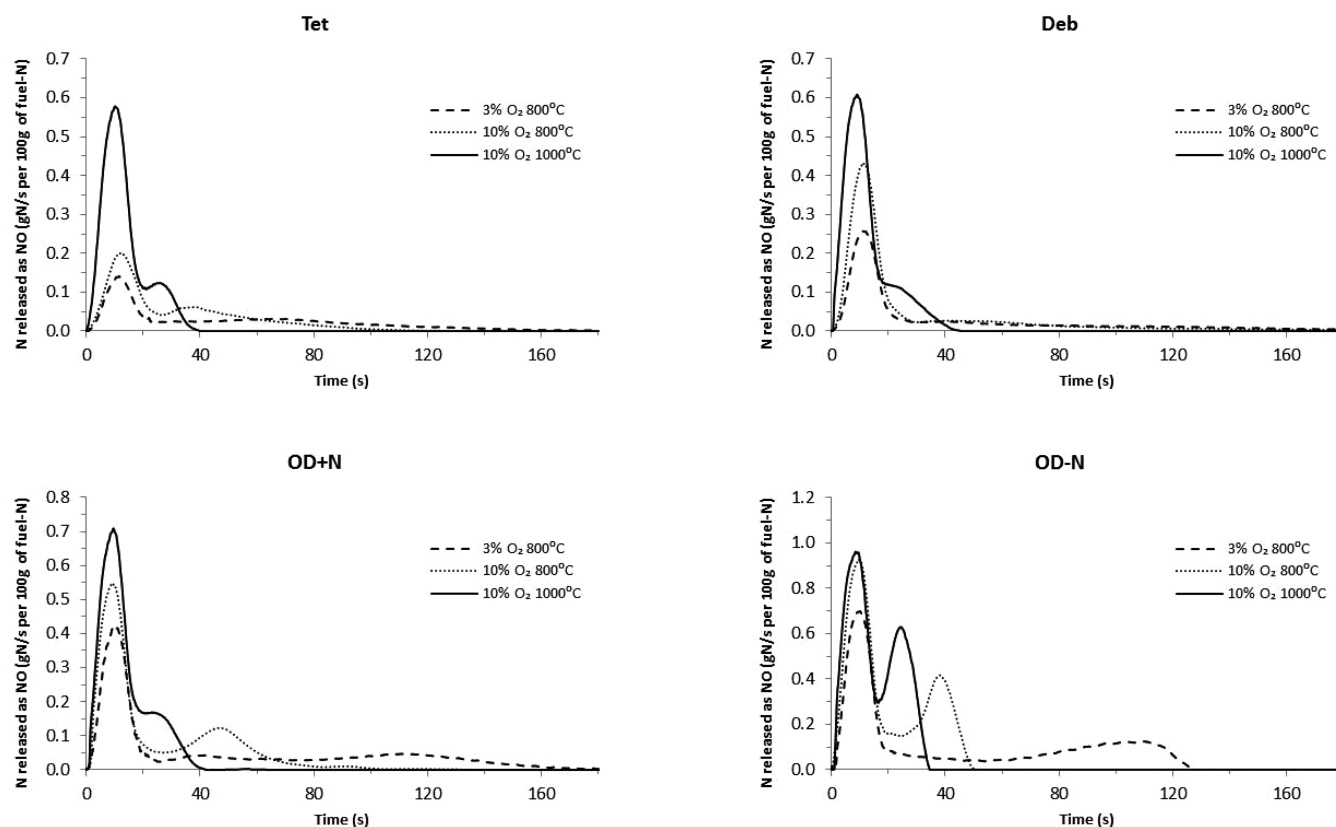
**3.1. Carbon Release.** Figure 3 shows the C conversion to CO and CO<sub>2</sub> for each of the tested algae in the quartz tube furnace. The profiles all consist of an initial peak followed by a tail. We interpreted the initial peak to correspond to fuel devolatilization and combustion of the volatiles and the tail to correspond to oxidation of the residual char. Increasing the furnace temperature from 800 to 1000 °C had a similar effect on the release profiles for all of the tested algae. The initial peaks were both higher and narrower at 1000 °C than at 800 °C, indicating an increase in the amount and rate of C conversion to CO and CO<sub>2</sub> during devolatilization at the higher temperature. The tails were shorter at 1000 °C and started from higher up on the peak, indicating an increase in the rate of char oxidation as well as greater overlap between devolatilization and char oxidation. The times necessary for carbon burnout were in the order of 25–35 s at 1000 °C and 40–90 s at 800 °C. Decreasing the oxygen partial pressure from 10 to 3 vol % resulted in a significant increase in the carbon burnout times for the tested algae, as indicated by the increase in tail lengths at the 3% O<sub>2</sub> and 800 °C reaction conditions. Burnout times were in the order of 80–160 s at 3% O<sub>2</sub> and 800 °C. As expected, char burnout times for Deb and OD + N, the two fuels with the highest FC contents, were greater than the burnout times for Tet and OD – N.

Figure 4 shows the C conversion to CO and CO<sub>2</sub> from the tested algae. Carbon conversion was determined by comparing the total C emitted as CO and CO<sub>2</sub> in the quartz tube furnace to the initial fuel C content reported in Table 1. As expected, the total release of carbon was proportional to the initial fuel C content. The C mass-balance closures were all within 84%. Unreacted light hydrocarbons most likely accounted for the balance, and therefore, for higher oxygen partial pressure and



**Figure 4.** Carbon conversion to CO and CO<sub>2</sub> from the tested algae as determined by oxidizing algae samples in a quartz tube furnace. Fuel C contents were taken from Table 1. Data are on a daf basis.

temperature, the extent of light hydrocarbons being oxidized to CO and CO<sub>2</sub> is increased and a higher extent of carbon conversion to CO and CO<sub>2</sub> is measured. Figure 4 also shows the partitioning of carbon between the devolatilization and char oxidation stages. For these data, we have determined the transition between devolatilization and char oxidation based on an extrapolation of the initial devolatilization peak; the area under this peak was then used to determine the amount of C released as CO and CO<sub>2</sub> during devolatilization. The total release of carbon as CO and CO<sub>2</sub> during char oxidation was then determined as the difference between total carbon release



**Figure 5.** Nitrogen released as NO from the tested algae in a quartz tube furnace. Release profiles obtained at 10 vol %  $O_2$  and 800 °C are compared to release profiles obtained at 3 vol %  $O_2$  and 800 °C and at 10 vol %  $O_2$  and 1000 °C.

(on the basis of the total area under the curve) and the total carbon release during devolatilization. The majority (53–73%) of the C released as CO and  $CO_2$  was emitted during devolatilization. This is expected given the high VM/FC ratios of the tested alga.

Reducing the oxygen partial pressure from 10 to 3%  $O_2$  resulted in a slight decrease in the proportion of C converted to CO and  $CO_2$  during devolatilization for all of the tested algae. This is again attributed to unconverted light hydrocarbons released during devolatilization. Increasing the furnace temperature from 800 to 1000 °C affected the C partitioning in different ways for the different algae. For Tet and Deb, an increasing temperature resulted in an increase in the proportion of carbon released as CO and  $CO_2$  during devolatilization, which is expected because of the known dependence of the volatile yield on the temperature. For OD + N and OD – N, an increasing temperature had the opposite effect on the C partitioning, and the reason for this is unclear. It is possible that there was some removal of carbon by the formation of soot at the higher temperature because of the increased rate of devolatilization.<sup>33</sup>

**3.2. Nitrogen Release.** Figure 5 shows the N released as NO from the tested algae in the quartz tube furnace. Similar to the carbon release profiles, the NO release profiles all consisted of an initial peak, presumably corresponding to fuel devolatilization and the homogeneous reaction of the released volatiles, and a tail, presumably corresponding to oxidation of the residual char. The initial peaks from the different algae vary in both height and width but, otherwise, are similar in shape. The shape of the tails on the other hand vary depending upon the alga and the reaction conditions, possibly indicating

different release mechanisms during char oxidation. The profiles corresponding to OD + N, OD – N, and to a lesser extent, Tet all contained at least one secondary peak. It is suspected that the secondary peaks are a result of changes in the char structure during char oxidation. It is possible that the changes in the char structure expose nitrogen-rich zones of the char matrix. While there were some small differences in the temporal responses of the gas analysers used to measure CO,  $CO_2$ , and NO, it is still clear that nitrogen burnout took longer than carbon burnout, indicating selective depletion of fuel C over fuel N. Nitrogen burnout times were of the order of 35–45 s at 10%  $O_2$  and 1000 °C, 50–220 s at 10%  $O_2$  and 800 °C, and 130–240 s at 3%  $O_2$  and 800 °C. Nitrogen burnout was fastest for OD – N, which contained the least fuel N, and was the slowest for Deb, the algae with the most fuel N. Nitrogen burnout times for Tet and OD + N were between those of OD – N and Deb. Nitrogen burnout took slightly longer for Tet than for OD + N, even though OD + N contained more fuel N than Tet on a dry basis. This is likely a result of mass transfer limitations in the Tet sample caused by its high ash content.

Figure 6 shows the N conversions to NO for the tested algae expressed as a proportion of the available fuel N. Nitrogen conversion to NO was determined by comparing the total amount of N emitted as NO in the quartz tube furnace to the initial fuel N content reported in Table 1. Emissions of nitrogenous species other than NO were not measured. NO emissions ranged between 0.4 and 0.8 g of N/100 g for the tested algae, corresponding to fuel N conversion to NO of 5.9–21.2% (Figure 6). The balance of fuel N was most likely emitted as other gas-phase nitrogenous species, including, for example,  $N_2$ ,  $NH_3$ , HCN, and  $N_2O$ . On average, Deb emitted



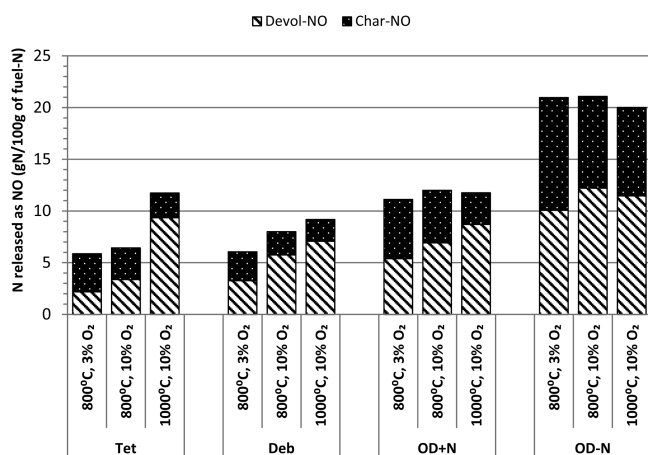


**Figure 6.** Nitrogen conversion to NO for the tested algae as determined by oxidizing algae samples in a quartz tube furnace. Fuel N contents were taken from Table 1.

the most NO (0.53 g of N/100 g, db) of the tested algae, followed by OD + N (0.48 g of N/100 g, db), OD – N (0.26 g of N/100 g, db), and then Tet (0.19 g of N/100 g, db). NO emissions from the macroalgae samples were found to increase with increasing fuel N content; however, the increase was not proportional to the increase in fuel N content. In fact, N conversion to NO diminished with increasing fuel N content on a daf basis. This trend may be attributed to thermal  $\text{deNO}_x$  involving the homogeneous reduction of NO by  $\text{NH}_3$  to  $\text{N}_2$  and  $\text{H}_2\text{O}$ .<sup>50</sup> Giuntoli et al.<sup>33</sup> explained that an increasing fuel N content leads to an increase in the concentration of  $\text{NH}_i$  radicals released during devolatilization, which results in an increase in the extent of NO reduction by thermal  $\text{deNO}_x$ . The same trend has been reported during the combustion of various types of terrestrial biomass;<sup>32–34</sup> however, this is less apparent

in coal combustion,<sup>32,51</sup> in which N conversion to NO seems relatively insensitive to the amount of fuel N. The results for the macroalgae (OD + N, OD – N, and Deb) are compared to the NO emission data reported by Giuntoli et al.<sup>33</sup> and Winter et al.<sup>34</sup> for terrestrial biomass in Figure 7. Winter et al.<sup>34</sup> measured NO emissions from spruce wood, alder wood, peat, and malt waste in a fluidized-bed reactor. Giuntoli et al.<sup>33</sup> measured NO emissions from five waste fuels in the same reactor used in the present study. The conversions reported by Winter et al.<sup>34</sup> are lower than the conversions reported in this study and by Giuntoli et al.;<sup>33</sup> however, this is likely to be due to the different reactor configurations.

Nitrogen released as NO from Tet was the most sensitive to changes in the temperature of all of the tested algae. At 800 °C and 10 vol %  $\text{O}_2$ , only 5.9% of the fuel N in Tet was converted to NO. The NO emission levels from Tet were 20% lower than the levels emitted by OD + N at 800 °C, even though the Tet sample contained nearly 50% more fuel N than OD + N on a dry basis. At 1000 °C, the amount of N released as NO from Tet almost doubled and exceeded that released by OD + N by approximately 50%. By comparing the heights of the initial peaks from the NO emission profiles for Tet at 800 and 1000 °C at 10 vol %  $\text{O}_2$  in Figure 5, it can be seen that the increase in NO emissions at 1000 °C occurred during devolatilization rather than during char oxidation. The N partitioning (as determined using the same method used to determine the C partitioning) for Tet shifted from 53% devolatile NO/47% char NO at 800 °C to 80% devolatile NO/20% char NO at 1000 °C, as illustrated in Figure 6. The increase in the temperature had a similar effect but to a lesser extent on the N partitioning for Deb and OD + N. The NO emissions from OD – N were relatively insensitive to the change in the temperature.

The amount of N released as NO from the tested algae was found to decrease by up to 32% upon reducing the oxygen partial pressure from 10 to 3 vol %  $\text{O}_2$ . The reduction in NO

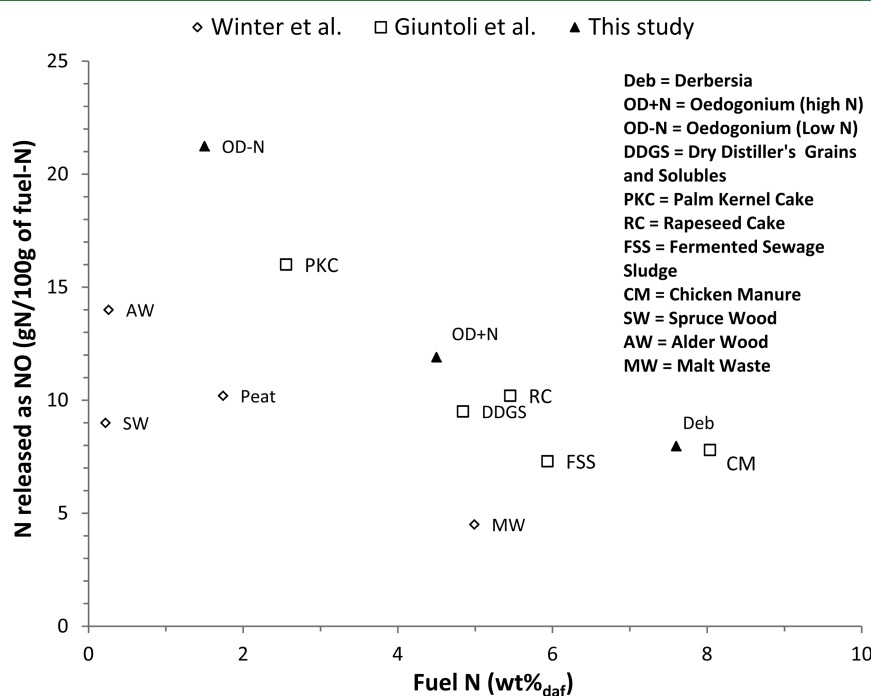


**Figure 7.** Fuel N conversion to NO as a function of initial fuel N content at 800 °C and 10%  $\text{O}_2$ . Data for the macroalgae samples are compared to data reported for terrestrial biomass by Giuntoli et al.<sup>33</sup> and Winter et al.<sup>34</sup>

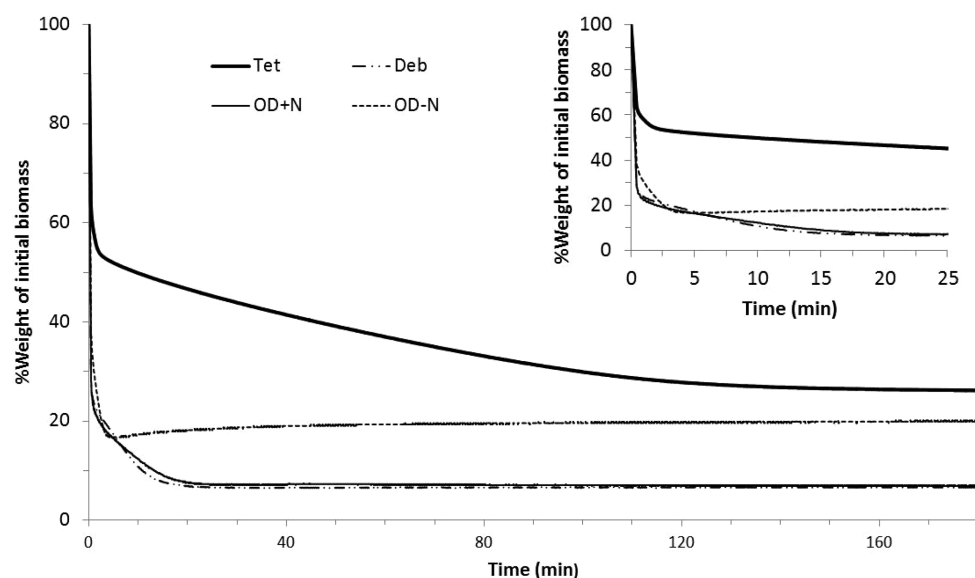


**Figure 8.** Gasification weight loss profiles for the tested algae at 800 °C in pure CO<sub>2</sub>. The sudden reduction in the slope of the weight loss curves indicates the transition between fuel devolatilization and oxidation of the residual char. The inset (small plot) shows the first 25 min of reaction.

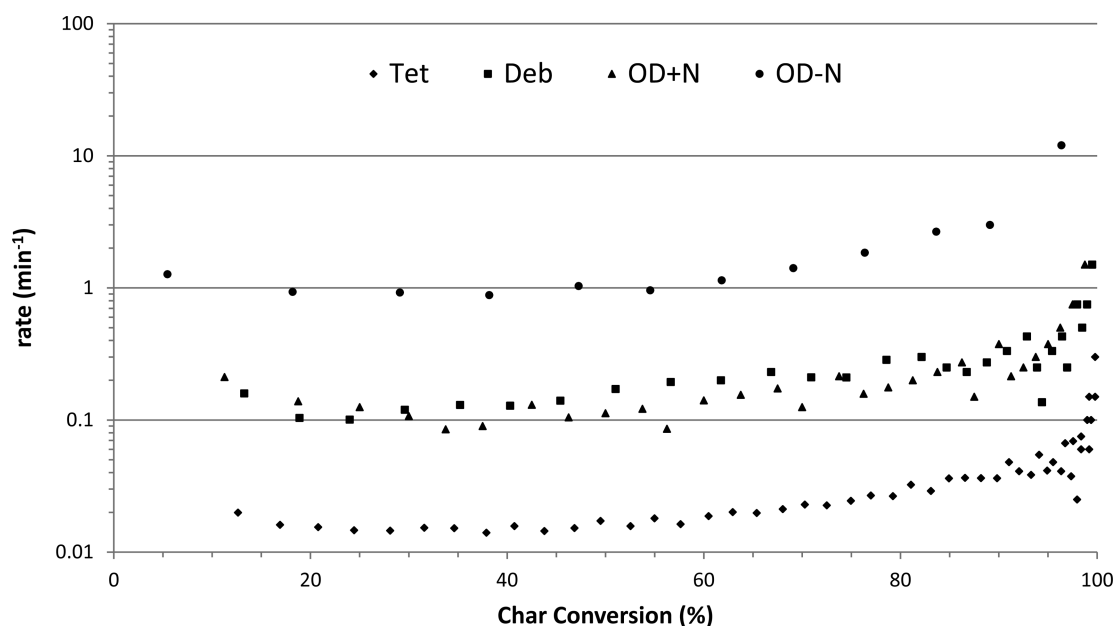


**Figure 9.** Char gasification rate profiles for the tested algae at 800 °C in pure CO<sub>2</sub>. The rate profiles were calculated from the gasification weight loss curves presented in Figure 8.

emissions occurred mainly during devolatilization, and consequently, the N-partitioning shifted away from devolatilization and toward char oxidation. This change in N-release behavior is consistent with results reported in the literature for both coal and biomass.<sup>32</sup> Jenkins et al.<sup>32</sup> explained that the reduced oxygen availability at lower oxygen partial pressures leads to increased competition for oxygen between C and N, resulting in reduced availability of oxygen for NO<sub>x</sub> formation. The NO release from OD – N was relatively insensitive to the change in oxygen partial pressure and was an exception to this finding.

**3.3. Char Reactivity.** The CO<sub>2</sub> gasification weight loss profiles for the tested algae are presented in Figure 8. Complete conversion of the chars took between 200 s and 2.5 h. Upon close inspection of Figure 8, the curve for OD – N reaches a

minima of 17% at approximately 200 s and then proceeds to increase to 20% (the steady-state value) with increasing time. When calculating the instantaneous rate ( $r''$ ) of char conversion for OD – N, the weight at the minima was used rather than the steady-state weight. The increase in sample weight after 200 s is most likely due to carbonate formation, resulting from the reaction of CO<sub>2</sub>, the gasifying agent, with inorganic elements (especially calcium) in the residual char. In the first 200 s of reaction, it is likely that there was a reduced concentration of CO<sub>2</sub> in the gaseous environment immediately surrounding the algae particles because of the presence of pyrolysis gases. This would have reduced the potential for carbonate formation.

The char of Tet was by far the least reactive of the tested algae, as seen by comparison of the rate profiles presented in Figure 9. The rate profiles show how the instantaneous reaction

rate changes with char conversion. The Tet char was approximately 1 order of magnitude less reactive than the chars from Deb and OD + N and 2 orders of magnitude less reactive than the OD - N char. The relatively low reactivity of the Tet char can also be seen in Figure 8. After 2 h, much of the Tet char was still unconverted, whereas the chars from Deb, OD + N, and OD - N were all more or less completely converted after 25 min. The reactivity of the Tet char is also significantly lower than that reported for *Chlorella* sp. microalgae by Kirtania et al.,<sup>43</sup> who found the char from *Chlorella* sp. to be more or less completely converted within 20 min.<sup>43</sup> Mass transfer limitations were most likely responsible for the low reactivity of the Tet char. Tet has an extremely high ash/FC ratio (>15). By comparison, the ash/FC values for the macroalgae samples and for *Chlorella* sp.<sup>43</sup> were between 0.5 and 2.7. It is suspected that the ash from the Tet sample formed a protective layer around the char particles, which inhibited gas contact with the char.

The chars from Deb and OD + N had similar reactivities and were approximately an order of magnitude less reactive than the OD - N char. Differences in the macroalgae ashes are likely to be largely responsible for the differences observed in the reactivities of the macroalgal chars. The overall catalytic effect of the ashes is likely to depend upon the relative proportions of the main-ash forming elements in the macroalgae, which were K, Na, Ca, Mg, Si, and Cl. OD - N, the alga with the most reactive char, contained the most alkali metals and alkaline earth metals, both of which are known to have a strong catalytic effect on char gasification.<sup>38–41</sup>

The rate profiles for the tested algae all follow a similar trend. The rate was found to remain relatively constant for char conversions up until about 60% and then increase by approximately an order of magnitude in the range from 60 to 100% conversion. Moilanen et al.<sup>52</sup> reported a similar trend from the gasification of birch wood pieces in 1 bar steam at 800 °C in an apparatus that also involved *in situ* devolatilization. Henriksen et al.<sup>41</sup> also found that the reaction rate increased at high conversion values during the gasification of straw chars at 800 °C. Interestingly, the reactivities of the birch wood char and straw char were of a similar magnitude to that of the chars from OD + N and Deb; however, direct comparison is difficult because of differences in the experimental setup and gas atmospheres between those experiments and the experiments reported here. Moilanen<sup>40</sup> proposed two reasons for an increasing reaction rate with char conversion: (i) an increasing catalyst/C ratio in the residual char with an increasing char conversion and (ii) an increasing char porosity with an increasing conversion, making more active sites available for gasification. An increasing reaction rate profile with conversion has positive implications for achieving high conversions in practical systems because complete conversion of the char particles is more likely provided that the residence times for the char particles in the reactor are sufficiently long.

A high-temperature pulverized fuel reactor may be a suitable technology for the conversion of Tet given its low char reactivity. This technology would also have the added advantage that the microalgae could be fed as a powder. However, the impact of the high ash content for Tet would need to be considered. The macroalgae on the other hand are more reactive than Tet and may be better suited in low-temperature fluidized-bed reactors.

## CONCLUSION

The combustion of *Tetraselmis*, *Derbersia*, and two types of *Oedogonium* in a fixed bed within a quartz tube furnace showed that most of the fuel C is converted to CO and CO<sub>2</sub> during devolatilization, with carbon conversion exceeding 84% for all of the tested algae. Nitrogen conversions to NO in the quartz furnace ranged between 6 and 12 g of N/100 g of fuel N for *Tetraselmis*, 6–9 g of N/100 g of fuel N for *Derbersia*, and 11–21 g of N/100 g of fuel N for the two *Oedogonium* variants on a daf basis. The fraction of fuel N that was released as NO during combustion of *Oedogonium* was reduced by 43–49% by starving the alga of essential nutrients during cultivation. In most cases, NO emissions were also predominately released during devolatilization, which is consistent with the high volatile matter content for these fuels. The chars from *Oedogonium* and *Derbersia* have similar gasification reactivities and are an order of magnitude more reactive than the *Tetraselmis* char. The reactivities of these chars are similar in magnitude to that of birch wood char and straw char. The gasification reactivity of the *Oedogonium* char was increased by starving *Oedogonium* of essential nutrients during cultivation. The reactivities of the algal chars all increase at high char conversions.

## AUTHOR INFORMATION

### Corresponding Author

\*E-mail: peter.ashman@adelaide.edu.au.

### Notes

The authors declare no competing financial interest.

## ACKNOWLEDGMENTS

The characterisation work was carried out at the Process Chemistry Centre of Åbo Akademi University, Finland, within FUSEC (2011–2014), a project financed by the National Technology Agency of Finland (TEKES) and industrial partners Andritz Oy, Metso Power Oy, Foster Wheeler Energia Oy, UPM-Kymmene Oyj, Clyde Bergemann GmbH, International Paper, Inc., and Top Analytica Oy Ab. Nikolai de Martini is acknowledged for his help in the treatment of the quartz furnace data, and Luis Bezerra and Peter Backman are acknowledged for their technical support in various aspects of this work. This research was supported under Australian Research Council's Linkage Projects Funding Scheme (Project LP100200616) with our industry partner SQC Pty Ltd. The project was also supported by the Australian Government through the Australian Renewable Energy Agency (ARENA) and the Advanced Manufacturing Cooperative Research Centre (AMCRC), funded through the Australian Government's Cooperative Research Centre Scheme. Andrew Cole and Marie Magnusson are acknowledged for the support in the production of macroalgal biomass. The authors also acknowledge the support of Muradel Pty Ltd. and MBD Energy.

## REFERENCES

- (1) Naik, S. N.; Goud, V. V.; Rout, P. K.; Dalai, A. K. *Renewable Sustainable Energy Rev.* **2010**, *14*, 578–597.
- (2) Obernberger, I.; Thek, G. *Biomass Bioenergy* **2004**, *27*, 653–669.
- (3) Skrifvars, B.; Backman, R.; Hupa, M.; Sfiris, G.; Åbyhammar, T.; Lyngfelt, A. *Fuel* **1998**, *77* (1), 65–70.
- (4) Werkelin, J.; Skrifvars, B.; Zevenhoven, M.; Holmbom, B.; Hupa, M. *Fuel* **2010**, *89*, 481–493.
- (5) Leckner, B.; Karlsson, M. *Biomass Bioenergy* **1993**, *4* (5), 379–389.

- (6) Piotrowska, P.; Zevenhoven, M.; Hupa, M.; Giuntoli, J.; de Jong, W. *Fuel Process. Technol.* **2013**, *105*, 37–45.
- (7) Steenari, B.; Lundberg, A.; Pettersson, H.; Wilewska-Bien, M.; Andersson, D. *Energy Fuels* **2009**, *23*, 5655–5662.
- (8) Boström, D.; Eriksson, G.; Boman, C.; Öhman, M. *Energy Fuels* **2009**, *23*, 2700–2706.
- (9) Öhman, M.; Nordin, A.; Lundholm, K.; Boström, D. *Energy Fuels* **2003**, *17*, 1153–1159.
- (10) Lynch, D.; Henihan, A. M.; Bowen, B.; Lynch, D.; McDonnell, K.; Kwapinski, W.; Leahy, J. J. *Biomass Bioenergy* **2013**, *49*, 197–204.
- (11) Chisti, Y. *Biotechnol. Adv.* **2007**, *25*, 294–306.
- (12) Pienkos, P. T.; Darzins, A. *Biofuels, Bioprod. Biorefin.* **2009**, *3* (4), 431–440.
- (13) Lawton, R. J.; de Nys, R.; Paul, N. A. *PloS One* **2013**, *8* (5), 1–7.
- (14) Borowitzka, L. J.; Borowitzka, M. A.; Moulton, T. P. *Hydrobiologia* **1984**, *116* (1), 115–121.
- (15) Brennan, L.; Owende, P. *Renewable Sustainable Energy Rev.* **2010**, *14*, 557–577.
- (16) Mulbry, W.; Kondrad, S.; Pizarro, C.; Kebede-Westhead, E. *Bioresour. Technol.* **2008**, *99* (17), 8137–8142.
- (17) Tsagakamilis, P.; Danielidis, D.; Dring, M. J.; Katsaros, C. *J. Appl. Phycol.* **2010**, *22*, 331–339.
- (18) Saunders, R. J.; Paul, N. A.; Hu, Y.; de Nys, R. *PloS One* **2012**, *7* (5), 1–8.
- (19) Ross, A. B.; Anastakis, K.; Kubacki, M.; Jones, J. M. *J. Anal. Appl. Pyrolysis* **2009**, *85*, 3–10.
- (20) Ross, A. B.; Jones, J. M.; Kubacki, M. L.; Bridgeman, T. *Bioresour. Technol.* **2008**, *99*, 6494–6504.
- (21) Ross, A. B.; Biller, P.; Kubacki, M. L.; Li, H.; Lea-Langton, A.; Jones, J. M. *Fuel* **2010**, *89* (9), 2234–2243.
- (22) Biller, P.; Ross, A. B.; Skill, S. C.; Lea-Langton, A.; Balasundaram, B.; Hall, C.; Riley, R.; Llewellyn, C. A. *Algal Res.* **2012**, *1*, 70–76.
- (23) Wang, S.; Jiang, X. M.; Han, X. X.; Wang, H. *Energy Fuels* **2008**, *22*, 2229–2235.
- (24) Wang, J.; Wang, G.; Zhang, M.; Chen, M.; Li, D.; Min, F.; Chen, M.; Zhang, S.; Ren, Z.; Yan, Y. *Process Biochem.* **2006**, *41*, 1883–1886.
- (25) Chakinala, A. G.; Brilman, D. W. F.; van Swaaij, W. P. M.; Kersten, S. R. A. *Ind. Eng. Chem. Res.* **2010**, *49*, 1113–1122.
- (26) Haiduc, A. G.; Brandenberger, M.; Suquet, S.; Vogel, F.; Bernier-Latmani, R.; Ludwig, C. *J. Appl. Phycol.* **2009**, *21*, 529–541.
- (27) Bird, M. I.; Wurster, C. M.; de Paula Silva, P. H.; Bass, A. M.; de Nys, R. *Bioresour. Technol.* **2011**, *102*, 1886–1891.
- (28) Glarborg, P.; Jensen, A. D.; Johnsson, J. E. *Prog. Energy Combust. Sci.* **2003**, *29*, 89–113.
- (29) Hansson, K.; Samuelsson, J.; Tullin, C.; Åmand, L. *Combust. Flame* **2004**, *137* (3), 265–277.
- (30) Chen, S. L.; Heap, M. P.; Pershing, D. W.; Martin, G. B. *Fuel* **1982**, *61*, 1218–1224.
- (31) Ashman, P. J.; Haynes, B. S.; Buckley, A. N.; Nelson, P. F. *Symp. (Int.) Combust., [Proc.]* **1998**, *27* (2), 3069–3075.
- (32) Jenkins, B. M.; Baxter, L. L.; Miles, T. R., Jr.; Miles, T. R. *Fuel Process. Technol.* **1998**, *54*, 17–46.
- (33) Giuntoli, J.; de Jong, W.; Verkooyen, A. H.; Piotrowska, P.; Zevenhoven, M.; Hupa, M. *Energy Fuels* **2010**, *24*, 5309–5319.
- (34) Winter, F.; Wartha, C.; Hofbauer, H. *Bioresour. Technol.* **1999**, *70*, 39–49.
- (35) Abelha, P.; Gulyurtlu, I.; Cabrita, I. *Energy Fuels* **2008**, *22*, 363–371.
- (36) Vassilev, S. V.; Baxter, D.; Andersen, L. K.; Vassileva, C. G. *Fuel* **2010**, *89*, 913–933.
- (37) Chen, C.; Ma, X.; Liu, K. *Appl. Energy* **2011**, *88*, 3189–3196.
- (38) Kannan, M. P.; Richards, G. N. *Fuel* **1990**, *69*, 747–753.
- (39) Spiro, C. L.; McKee, D. W.; Kosky, P. G.; Lamby, E. J. *Fuel* **1983**, *62*, 180–183.
- (40) Moilanen, A. Thermogravimetric characterisations of biomass and waste for gasification processes. Doctoral Thesis, Åbo Akademi University, Turku, Finland, 2006.
- (41) Relationship between gasification reactivity of straw and water soluble compounds present in this material. In *Developments in Thermochemical Biomass Conversion*; Bridgwater, A. V., Boocock, D. G. B., Eds.; Blackie Academic and Professional: London, U.K., 1997; Vol. 2, pp 881–891.
- (42) Hupa, M. *Energy Fuels* **2012**, *26*, 4–14.
- (43) Kirtania, K.; Joshua, J.; Kassim, M. A.; Bhattacharya, S. *Fuel Process. Technol.* **2014**, *117*, 44–52.
- (44) Lee, A. K.; Lewis, D. M.; Ashman, P. J. *Bioresour. Technol.* **2013**, *128*, 199–206.
- (45) Demirbaş, A. *Fuel* **1997**, *76* (5), 431–434.
- (46) Mani, S.; Tabil, L. G.; Sokhansanj, S. *Biomass Bioenergy* **2004**, *27*, 339–352.
- (47) Giuntoli, J.; de Jong, W.; Arvelakis, S.; Spliethoff, H.; Verkooyen, A. H. M. *J. Anal. Appl. Pyrolysis* **2009**, *85*, 301–312.
- (48) Wang, X.; Jin, Y.; Wang, Z.; Mahar, R. B.; Nie, Y. *J. Hazard. Mater.* **2008**, *160*, 489–494.
- (49) Healey, F. P. *Crit. Rev. Microbiol.* **1973**, *3* (1), 69–113.
- (50) Kasuya, F.; Glarborg, P.; Johnsson, J. E.; Dam-Johansen, K. *Chem. Eng. Sci.* **1995**, *50* (9), 1455–1466.
- (51) Gavin, D. G.; Dorrington, M. A. *Fuel* **1993**, *72*, 381–388.
- (52) Gasification reactivity of large biomass pieces. In *Science in Thermal and Chemical Biomass Conversion*; Bridgwater, A. V., Boocock, D. G. B., Eds.; CPL Press: Newbury, U.K., 2006; Vol. 1, pp 509–518.